A&A 481, 253–258 (2008)
DOI: 10.1051/0004-6361:20079182

Astronomy & Astrophysics

Sub-hour modulation of L-component of Io-related Jovian decametric emission⋆

O. V. Arkhypov[1] and H. O. Rucker[2]

[1] Institute of Radio Astronomy, National Academy of Sciences of Ukraine, Chervonopraporna 4, 61002 Kharkiv, Ukraine
e-mail: rai@ri.kharkov.ua
[2] Space Research Institute, Austrian Academy of Sciences, Schmiedlstrasse 6, 8042 Graz, Austria
e-mail: rucker@oeaw.ac.at

Received 3 December 2007 / Accepted 10 January 2008

ABSTRACT

The variability of Jovian decametric emission (DAM) is studied at time scales from 1 min to 1 h with DAM records of 1991–2007 from the archive of Nancay Radio Observatory. We found that the internal structure of the Io-related radio storms has the dominating periodicity of 23±2 min on average. This estimate practically coincides with the fundamental eigenoscillations of transversal magnetic pulsations in the Io plasma torus. Our autocorrelation analysis confirms the excess of DAM variations with the time scale of the fundamental and first harmonic periods of the Io torus. Moreover, the time scale of arc pattern in DAM dynamic spectra is estimated to be 5.4 min, which corresponds to Io's Alfvén wing diameter or to the 3rd and 4th harmonics of torus proper oscillations. These results could be interpreted in terms of electron acceleration in field-aligned electric fields of standing Alfvén waves trapped in the Io torus. There is an analogous modulation of auroral kilometric radiation of the Earth by magnetic pulsations at field line resonances in the terrestrial magnetosphere (Hanasz et al. 2006, J. Geophys. Res., 111, A03209).

Key words. planets and satellites: individual: Jupiter – radio continuum: solar system – magnetohydrodynamics (MHD) – waves – radiation mechanisms: non-thermal – plasmas

1. Introduction

Jovian decametric emission (DAM) appears mainly in the form of long (*L*) bursts with the time scale of ∼1 s. Such modulation is a result of emission scattered in the interplanetary medium (Genova & Leblanc 1981) and inner magnetosphere of Jupiter (Arkhypov & Rucker 2007). The terrestrial ionosphere creates DAM flux variability with quasi-periods of 10 to 70 s (Genova et al. 1981). DAM flux variations with time scales of 1 to 10 h are the product of Jupiter rotation (Galopeau et al. 2004) and Io orbital motion (Bigg 1964). All such modulations are studied in detail. However, the phenomenology and origin of DAM variations on intermediate scales (1 to 60 min) are poorly understood.

Such sub-hour modulations are described as arcs of emission in DAM dynamic spectra (Leblanc 1981). The shapes of these arcs, as well as their spectral and polarization properties, have attracted researchers' attention (e.g.: Queinnec & Zarka 1998; Shaposhnikov et al. 2000). Usually, arcs are repeated quasi-periodically (Fig. 1). However, their time scale was studied only visually with old Voyager-1, 2 data (Leblanc 1981; Staelin et al. 1988). It was found that arcs are concentrated in groups, which were associated with Alfvén wings from Io (Gurnett & Goertz 1981; Bagenal & Leblanc 1988). However, the intervals between individual arcs are too brief (Leblanc & Bagenal 1990). To explain this discrepancy, Wright (1987) suggested the Io Alfvénic excitation of higher harmonic eigenmodes of the satellite's magnetic shell as a stimulator of DAM.

In addition, various studies noted the modulation of DAM by short-wavelength hydromagnetic (MHD) waves in Jovian magnetosphere (Arkhypov & Rucker 2006, 2007; Ergun et al. 2006). The most likely mechanism explaining DAM is the electron-cyclotron maser instability (Zarka 1998). It can thus be expected that DAM flux pulsations are related to periodic field-aligned electric fields provided by Alfvén waves, which accelerate electrons and stimulate plasma instabilities with electromagnetic wave generation. There are many arguments for this connection.

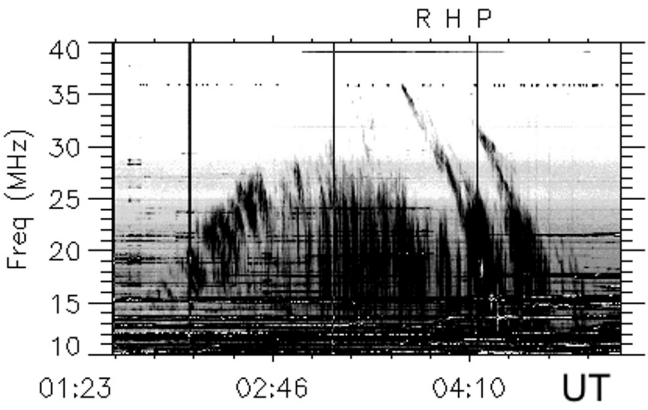

Fig. 1. An example of DAM dynamic spectra with clear arc pattern is recorded 2000 September 26 in the Nancay Radio Observatory.

Ergun et al. (2006) argued in detail for the connection of short (S-) bursts of DAM with short-scale Alfvén waves in the Jovian ionospheric resonator. Some signs of DAM modulations by a standing Alfvén wave have indeed been found recently in the Jovian ionosphere, such as the system of S-burst bands in the dynamic spectrum (Arkhypov & Rucker 2006). Another

⋆ Table 1 is only available in electronic form at http://www.aanda.org

modulation effect is the system of periodic peaks (or eigenfrequencies of the ionospheric Alfvén resonator) in the power spectra of low frequency oscillations of S-emission flux.

Hanasz et al. (2006) found that Alfvénic vibrations of magnetic field lines are able to drive pulsations of terrestrial kilometric radiation. It follows, from correlated observations made by the Interball-2 spacecraft and the IMAGE magnetometer array, that such radio pulsations often occur (in 39 out of 61 cases) simultaneously with field line resonances, and at frequencies near to those of vibrations. There is an analogy between terrestrial kilometric radiation and Jovian DAM, which are considered parts of the common phenomenon "*auroral radio emission*" of magnetized planets (Zarka 1998).

Jovian satellite Io is a powerful generator of Alfvén waves due to its high volcanic activity and the dense plasma torus from volcanic ejections around its orbit (Neubauer 1980; Goertz 1980; Belcher 1987). The Io torus represents a low Alfvén velocity channel that may give rise to ducted wave propagation as well as cavity resonances. Such magnetic pulsations were found in situ (Glassmeier et al. 1989). Corresponding field-aligned electric fields of standing Alfvén waves can modulate the electron flux and the related DAM. Therefore, the eigenfrequencies of the Io torus as a waveguide may be imprinted in DAM flux variations, which could be used for plasma remote sensing.

Thus far, DAM variations at sub-hour time scale have been studied visually with very limited experimental material from Voyager missions (Leblanc 1981; Leblanc & Bagenal 1990; Wright & Smith 1990), or with the ground-based, low-sensitivity, dipole antenna at one frequency (Wilkinson 1998). In these studies, the main approach is a statistical analysis of time intervals between DAM arcs. Unfortunately, such interval methods are not adequate for any study of arc groups that are divided into brief inter-arc intervals.

We study the DAM modulations with objective, more effective spectral and correlation methods using the archive of 17-yr broadband DAM observations at the Nancay Radio Observatory. Our purpose is to reveal DAM sub-hour modulations to compare them with the Io torus eigenfrequencies.

The methods and experimental material are described in Sect. 2. Section 3 describes our analysis of the DAM spectra. The promising interpretations are considered in Sect. 4. Section 5 summarizes the results.

2. Experimental material and methods

We used the collection of quicklook DAM spectra from the site of the Nancay Radio Observatory (http://www.obs-nancay.fr/dam/a_rapdam.htm). All data for every observational session are displayed separately as a pair of dynamic spectra for right-hand (RH) and left-hand (LH) polarization. The time coverage (8 h) and resolution (generally 40 s per pixel) of the spectra are quite sufficient for the study of DAM variations with periods from 2 h to minutes.

As the calibration of individual spectra is not published, only relative intensity could be analyzed. The intensity is coded in color on the spectrum. In RGB coding, the red (R) channel shows powerful interference, while the blue one (B) depicts mainly the antennae/amplifier noise. The most informative is the green (G) channel, which shows DAM storms in details. That is why for our analysis we usually used spectra in G-channel as grey images in 256 gradations (Fig. 1).

The purpose of this paper is the estimate of the main time scale of the interior structure inside a DAM storm. To avoid interference and modulation of DAM from the Jovian rotation, we cut out the radio storm of the dynamic spectrum. The borders of such storm clippings are listed in Table 1. This spectral fragment is rectangular in shape and one covers the whole region with Io-related radio emission at minimal interference.

Then, we calculated the squared harmonics of Fourier transform from the time variations of spectral intensity:

$$C_m^2 = A_m^2 + B_m^2, \tag{1}$$

$$A_m = \frac{1}{N}\sum_{i=1}^{N} F_i \cos\frac{2\pi mi}{N}, \tag{2}$$

$$B_m = \frac{1}{N}\sum_{i=1}^{N} F_i \sin\frac{2\pi mi}{N}, \tag{3}$$

where m is the harmonic number; N is the number of all intensity readings (F_i) in the spectrum; i is the intensity reading number. Such power estimates C_m^2 are obtained at each radio frequency of the spectral fragment and averaged into $\langle C_m^2\rangle$ with the standard error σ. As the number of radio frequency channels is 24 to 121, parameter σ practically describes the Gaussian statistic of $\langle C_m^2\rangle$ reasonably well. The key parameter in our future analysis is the period $P = T/m$ of the spectral peak with maximal $\langle C_m^2\rangle$ and significant ($>3\sigma$) amplitude relative to the adjacent minima. In fact, this period P describes the time scale of the interior structure inside a DAM storm.

Unfortunately, any well-known arc structure of DAM storms does not dominate in the described power spectra. No spectral peak could be found in the case of irregular patterns. Therefore, the Fourier transform must be supplied with the correlation approach. This is the calculation of the average autocorrelation function of spectral intensity $F_{i,k}$

$$r_a(\Delta k) = \frac{1}{n}\sum_{i=1}^{n}\sum_{k=1}^{m}\frac{[F_{i,k} - \langle F\rangle_i][F_{i,k+\Delta k} - \langle F\rangle_i]}{m\sigma_i^2}, \tag{4}$$

where: i and k are the pixel numbers in the frequency and time scales; m and n are the width and height of the analyzed dynamic spectrum; Δk is a time shift in pixels; $\langle F\rangle_i$ is the average spectral intensity along the spectral line at constant i or radio frequency; σ_i is the dispersion of the spectral intensity on the line.

Examples of the main types of autocorrelation function are shown in Fig. 2, where the time shift in seconds is displaced instead of Δk. There are common features for different types of autocorrelation pattern. At first, the narrow-peak, near-zero shift reflects the short-duration details in the DAM dynamic spectrum. Hence, the peak width (Δt) is controlled by the arc duration in time at fixed frequency. The arc groups appear as a bell-like "pedestal" under the peak of their autocorrelation function (Figs. 2b, d, f). Therefore, the pedestal width (ΔT) is an estimate of the time scale or period of arc groups. The autocorrelation minimum or the inflection point with $d^2r_a/d\tau^2 = 0$ between the peak and the pedestal are used as formal borders to estimate Δt and ΔT (Fig. 2f).

3. Analysis

The survey of DAM dynamic spectra from the Nancay Jovian archive reveals the existence of specific modulation with the time scales of deca-minutes (Fig. 3). To visualize such macro-patterns, we smoothed the spectral intensity in each frequency channel to remove individual arcs and to retain larger details. These details are contrasted using black-white schemes

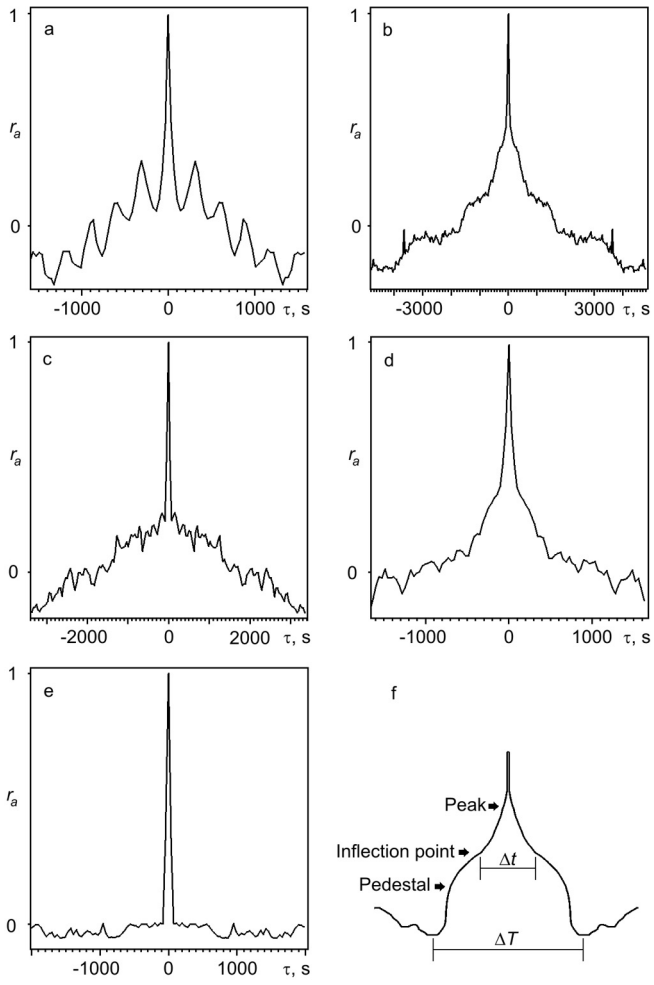

Fig. 2. The main types of the autocorrelation function of spectral intensity in Io-A radio storms: **a)** the periodic single arcs (2000 October 27); **b)** the periodic groups of arcs (2001 October 31); **c)** irregularly spaced single arcs (2005 February 10); **d)** irregularly spaced groups of arcs (2005 January 27); **e)** the background noise with low level of interference (2001 November 2007); **f)** the idealized scheme of measurements for the time scale of arcs (Δt) and arc groups (ΔT) on the central details of the function.

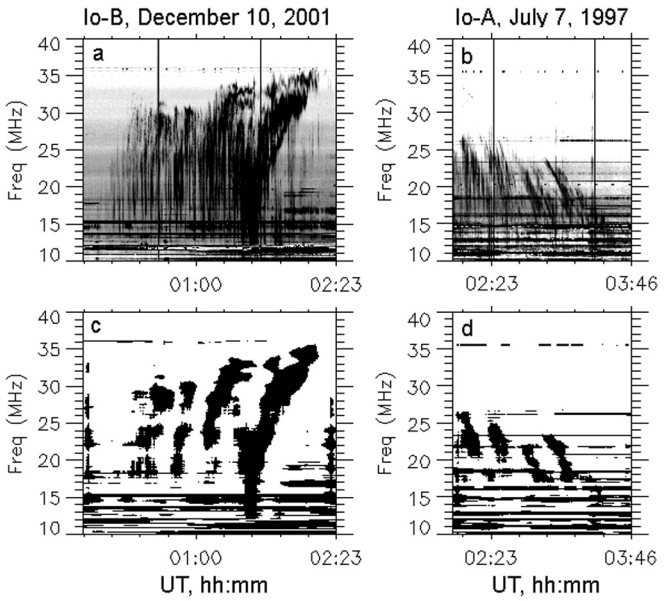

Fig. 3. Examples of DAM dynamic spectra with arc grouping in periodic macro-structures of deca-minute time scale: **a)**, **b)** the original spectra (Nancay Radio Observatory archive; right-hand polarization); **c)**, **d)** the visualization of macro-patterns.

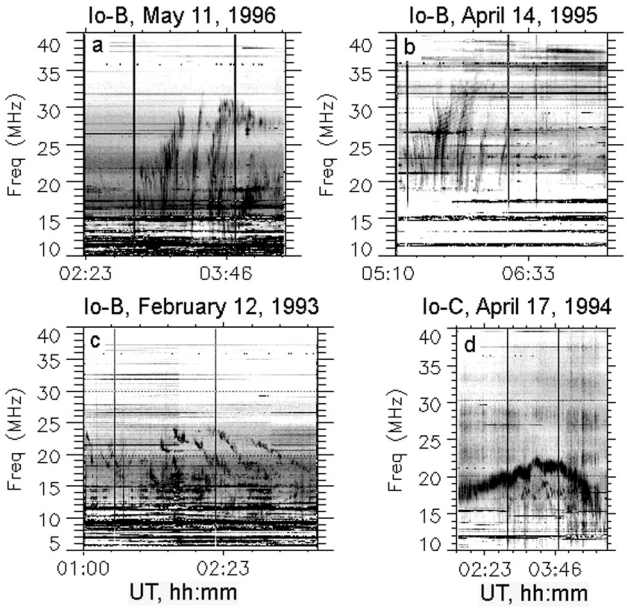

Fig. 4. Other types of deca-minute DAM modulation: **a)–c)** isolated arcs (Nancay Radio Observatory archive; right-hand polarization channel); **d)** undulations of the Io-C arc (Nancay Radio Observatory; left-hand polarization channel).

(Figs. 3c,d). There are other forms of such modulations: isolated arcs (Figs. 4a–c) and undulations of Io-C arc (Fig. 4d).

To find the dominating time scale in DAM storms, we applied Fourier transform (see details in Sect. 2). For each radio storm, the power spectrum of DAM fluctuations with time is calculated, and the significant peak with maximal power was found. The period P of the corresponding spectral harmonic is an individual estimate of the dominating scale. These estimates are concentrated just in the range of deca-minutes for all types of radio storms (Fig. 5). The average period is $\langle P \rangle = 1403 \pm 102$ s or 23 ± 2 min.

The time scale $\langle P \rangle$ we obtained is approximately that of the main eigenoscillations of the Io plasma torus. Glassmeier et al. (1989) found theoretically, for toroidal (transverse) magnetic oscillations in the Io torus, fundamental and first harmonic periods of 1296 s and 786 s, respectively (marked in Fig. 5). There is good agreement with the experimental histogram. Transverse Alfvén waves have field-aligned electric fields to accelerate electrons and modulate related DAM. Such proper magnetic oscillations with a period of 1200 s (20 min) are confirmed with Voyager-1 in situ magnetometer measurements (Glassmeier et al. 1989).

Our autocorrelation analysis confirms an excess of DAM variations with a time scale similar to the fundamental and first harmonic periods of the Io torus. Thus, Fig. 6 shows that the histogram of ΔT estimates has the maximum at $631 < \Delta T < 1585$ s. This is in accordance with calculations of the basic eigenoscillations of the Io torus (Glassmeier et al. 1989), and 15-min DAM modulation found by Wilkinson (1998).

As the correlation between ultraviolet emission of the Io torus and solar activity is discussed (Thomas 1993), we used

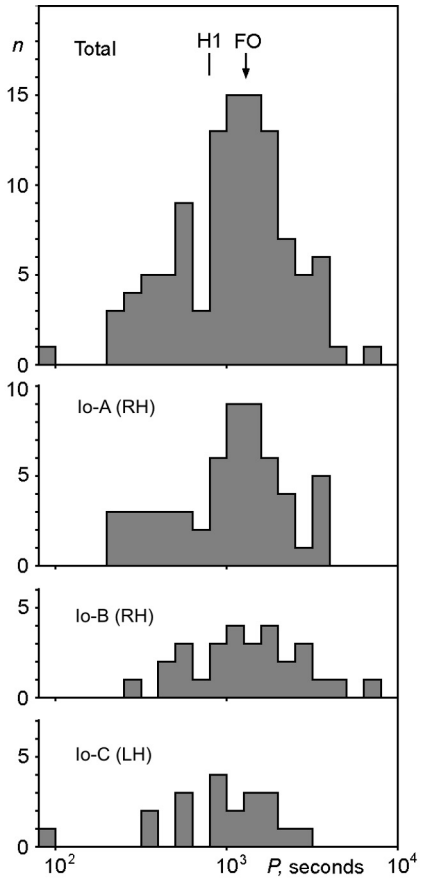

Fig. 5. Histograms of the dominating time scale of radio-storm interior structure in a dynamic spectrum of DAM. The fundamental period of transverse magnetic oscillations in the Io torus (FO) and the first harmonic (H1) are marked according to Glassmeier et al. (1989). The standard classification of DAM storm is used with the polarization channel in the brackets.

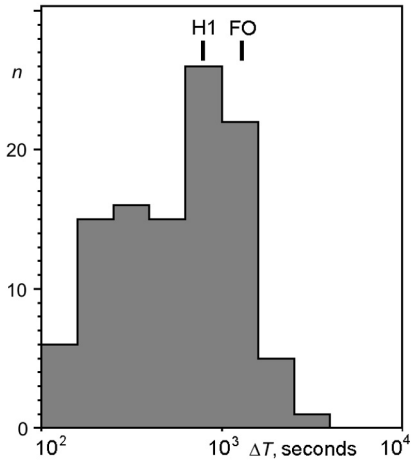

Fig. 6. The histogram of the ΔT estimates (i.e. arc group duration) shows an excess of DAM variations with time scales similar to the fundamental (FO) and first harmonic (H1) periods of transversal Alfvénic oscillations in the Io torus, according to Glassmeier et al. (1989).

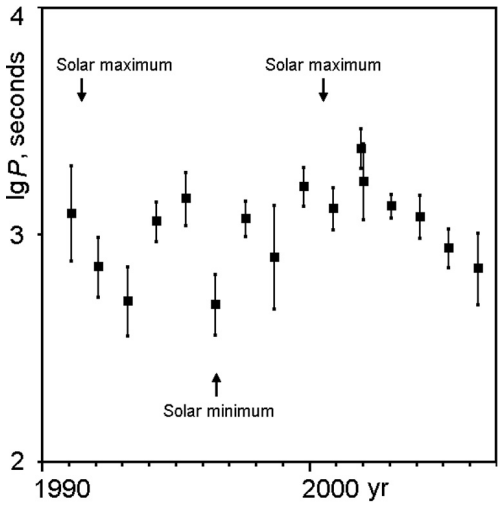

Fig. 7. Variations of the yearly estimate of the dominating time scale in DAM storm structure.

Fourier transforms to calculate the average time scale of radio storm structure for each year (Fig. 7). Although there is some coincidence of maximal and minimal P estimates with extremes of the annual sunspot number, the correlation coefficient $r = +0.44 \pm 0.20$ is rather uncertain. If daily sunspot numbers (SIDC data; http://sidc.oma.be/html/sunspot.html) are used with 107 individual P estimates, then the correlation vanishes ($r = +0.15 \pm 0.10$).

To estimate the scale of DAM arc pattern, we use the histogram of the width Δt of the autocorrelation main peak (Fig. 2f). The processing of noise fragments (without the DAM) of the same dynamic spectra (e.g., Fig. 2e) argues for the minimal Δt estimate of about 3 min, although one pixel on the dynamic spectra is about 0.7 min. As a result, the summary histogram of Δt estimates for DAM spectra from the table is shown in Fig. 8. Eighty-two percent of the estimates are concentrated in the interval $4.0 < \Delta t < 7.9$ min, with the average value $\langle \Delta t \rangle = 322 \pm 1$ s or 5.4 min. This result correlates with the old visual estimates for Io-related emission: 1–10 min (Leblanc 1981); 4–7 min (Staelin et al. 1988).

4. Discussion

It is suggested that arcs are the radio emissions that are stimulated by the system of the Io's Alfvén wings (e.g., Bagenal & Leblanc 1988; Queinnec & Zarka 1998). We would like to first draw attention to an interesting coincidence. During the obtained time scale of an arc ($\langle \Delta t \rangle = 5.4$ min), Io, with its system of Alfvén disturbances, displaces itself in the observer's rest frame over a distance of $V\langle \Delta t \rangle = 5605$ km or 3.08 $R_{\rm Io}$, where $V = 17.3$ km s^{-1} is the Io's orbital velocity, and $R_{\rm Io} = 1821$ km is the Io's radius. This 3 $R_{\rm Io}$ displacement practically coincides with the effective diameter of Io with its ionosphere as a conductor (2.8 $R_{\rm Io}$; Linker et al. 1998, plate 3 and 4) as well as with the width of the Io's Alfvén wing (2–4 $R_{\rm Io}$; Jacobsen et al. 2007, Fig. 2). As the Alfvénic parallel electric field can accelerate electrons and stimulate DAM (Bagenal & Leblanc 1988; Queinnec & Zarka 1998), this coincidence does not appear accidental.

Logically, $\langle \Delta t \rangle = 5.4$ min is the typical time for the observer's crossing through narrow radio beams emitted at fixed frequency from different magnetic tubes activated by one Alfvén disturbance. Apparently, the longitudinal dimension of this disturbance, $\Delta\lambda_{\rm a} \approx 3\ R_{\rm Io}/A_{\rm Io} = 0.013$ rad, controls the duration of DAM observation: $\Delta t = P_{\rm Io}\Delta\lambda_{\rm a}/2\pi \approx 5.3$ min, where $A_{\rm Io} = 421\,600$ km is the Io's orbit radius; $P_{\rm Io} = 2548$ min is the

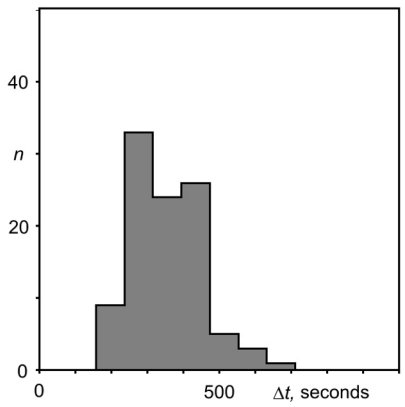

Fig. 8. The histogram of the Δt estimates shows the time scale of the arc pattern at fixed frequencies from 10 MHz to 35 MHz.

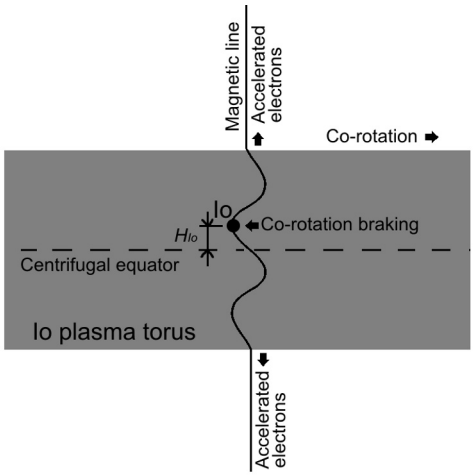

Fig. 9. Io can excite the resonance oscillations in 3rd harmonic of the Io plasma torus (grey band) during the most powerful DAM storms, when Io's position coincides with the maximum of the standing Alfvén wave. This Alfvén wave can accelerate electrons and modulate related DAM with periods of 5–6 min.

Io orbital period. However, this interpretation requires elementary radio beams much narrower than $\Delta\lambda_a \sim 0.7^o$.

Moreover, the bounce period of Io's Alfvén wings is about $P_b = 23$ min in the plasma rest frame (Bagenal & Leblanc 1988). However, the period in the observer's rest frame is too long: $360°\omega_c/(\omega\omega_I) = 75.5$ min; where $\omega = 360°/P_b = 15.65$ deg/min; $\omega_c = 0.4641$ deg/min is the angular frequency of the plasma co-rotation past Io; and $\omega_I = 0.1414$ deg/min is the Io's orbital angular velocity (Wright & Smith 1990). Hence, the problem of 20 min- and 5 min-periodicities (Figs. 1 and 2a) is still unresolved.

An alternative interpretation is the proper oscillation of the Io torus in the form of a quasi-axisymmetric azimuthal twisting of magnetic field lines intersecting the torus. Such oscillations are found in situ (Glassmeier et al. 1989). In this geometry, the phase of the torus oscillation negligibly depends on the longitude. Therefore, the observable period is identical to the torus eigenmode. The fundamental period for Alfvén waves in the torus is found experimentally to be about 20 min (Glassmeier et al. 1989), close to our time scale estimate for arc groups (23 min). Hence, the 5 min-periodicity could be considered as a 3rd harmonic with a period of about $P_3 = (23 \text{ min})/(1 + m) = 5.75$ min at $m = 3$. Smith & Wright (1989) numerically calculate that the toroidal 3rd harmonic has the angular frequency of (4.5009 rad)/(4.76 min) and the period of 6.64 min in the plasma rest frame of their model, indeed not far from the arc scale.

The effective excitation of the 3rd harmonic could be explained by the proximity of its standing wave maximum to Io's altitude above the centrifugal equator of the torus (Fig. 9). Thus Io stimulates the most intense DAM (Io-A, B) at the planetographical longitudes $\lambda \sim 200°$, where the satellite's altitude is $H_{Io} \sim (2/3)\alpha A_{Io} = 0.5R_J$. Here, $R_J = 71\,372$ km is the Jovian equatorial radius; $\alpha = \pi/2 - \arccos[\sin\theta_m \cos(\lambda - \lambda_m)]$ is the angle between planetocentric radius-vector of Io and the magnetic equator with the magnetic dipole longitude $\lambda_m = 159.2°$ and co-latitude $\theta_m = 9.5°$, according to the VIP4 model (Khurana et al. 2004). The factor 2/3 arises from the centrifugal force in the dipole geometry. The obtained H_{Io} is about the altitude of standing wave maximum $P_3 V_A/4 = 0.48R_J$ with the typical Alfvén velocity $V_A = 400$ km s^{-1} in the core of Io torus (Su et al. 2006).

The 4th harmonic with a period of about 5.19 min (Smith & Wright 1989; Wright & Smith 1990) could be effectively excited at $H_{Io} \sim 0$ during Io-C storms ($\lambda \geq 240°$). The most probable mechanism of such excitation is the spontaneous volcanic mass loading and subsequent co-rotation braking as argued by Glassmeier et al. (1989).

Therefore, the torus proper oscillations seem a promising candidate in the explanation of periodic DAM arcs, but some arcs can be of Alfven wing origin.

5. Conclusions

The processing of new observational material, covering 17 years, let us derive the following results.

1. It is found that the internal structure of the Io-related radio storms has the dominating periodicity of 23 ± 2 min on average. This estimate practically coincides with the fundamental mode of the Io torus eigenoscillations.
2. The autocorrelation analysis reveals an excess of emission variations with a time scale similar to the fundamental and first harmonic periods of Io's torus.
3. The time scale of arc pattern in DAM dynamic spectra is estimated to be 5.4 min, which corresponds to Io's Alfvén wing diameter or to the 3rd and 4th harmonics of torus eigenoscillations excited by Io.
4. These results could be interpreted in terms of electron acceleration in field-aligned electric fields of standing Alfvén waves trapped in the Io torus, with the torus acting as a resonator.

Hence, DAM could be used for remote monitoring of the Io torus resonances and its related plasma density.

References

Arkhypov, O. V., & Rucker, H. O. 2006, A&A, 452, 347
Arkhypov, O. V., & Rucker, H. O. 2007, A&A, 474, 1031
Carr, T. D., Desch, M. D., & Alexander, J. K. 1983, Phenomenology of magnetospheric radio emissions, in: Physics of the Jovian magnetosphere, ed. A. J. Dessler (Cambridge: Cambridge University Press), 226
Bagenal, F., & Leblanc, Y. 1988, A&A, 197, 311
Belcher, J. W. 1987, Science, 238, 170
Bigg, E. K. 1964, Nature, 203, 1008
Ergun, R. E., Su, Y.-J., Andersson, L., et al. 2006, J. Geophys. Res., 111, A6, A06212, doi: 10.1029/2005JA011253

Galopeau, P., Boudjada, M., & Rucker, H. 2004, J. Geophys. Res., 109, A12, A12217, doi: 10.1029/2004JA010459
Genova, F., & Leblanc, Y. 1981, A&A, 98, 133
Genova, F., Aubier, H. G., & Lecacheux, A. 1981, A&A, 104, 2, 229
Glassmeier, K.-H., Ness, N. F., Acuna, M. H., & Neubauer, F. M. J. 1989, J. Geophys. Res., 94, A11, 15063
Goertz, C. K. 1980, J. Geophys. Res., 85, A6, 2949
Gurnett, D. A., & Goertz, C. K. 1981, J. Geophys. Res., 86, A2, 717
Hanasz, J., de Feraudy, H., Schreiber, R., & Panchenko, M. 2006, J. Geophys. Res., 111, A03209
Jacobsen, S., Neubauer, F. M., Saur, J., & Schilling, N. 2007, Geophys. Res. Lett., 34, 10, doi: 10.1029/2006GL029187
Khurana, K. K., Kivelson, M. G., Vasyliunas, V. M., et al. 2004, in Jupiter: The Planet, Satellites and Magnetosphere, ed. F. Bagenal, T. E. Dowling, & W. B. McKinnon (Cambridge: Cambridge University Press), 593
Leblanc, Y. 1981, J. Geophys. Res., 86, A10, 8546
Leblanc, Y., & Bagenal, F. 1990, Adv. Space Res., 10, 49
Linker, J. A., Khurana, K. K., Kivelson, M. G., & Walker, R. J. 1998, J. Geophys. Res., 103, E9, 19867
Neubauer, F. M. 1980, J. Geophys. Res., 1980, 85, 1171
Queinnec, J., & Zarka, P. 1998, J. Geophys. Res., 103, A11, 26649
Shaposhnikov, V. E., Rucker, H. O., & Zaitsev, V. V. 2000, A&A, 355, 2, 804
Smith, P. R., & Wright, A. N. 1989, Nature, 339, 6224, 452
Staelin, D. H., Garnavich, P. M., & Leblanc, Y. 1988, J. Geophys. Res., 93, A5, 3942
Su, Y.-J., Jones, S. T., Ergun, R. E., et al. 2006, J. Geophys. Res., 111, A6, A06211, doi: 10.1029/2005JA011252
Thomas, N. 1993, J. Geophys. Res., 98, E10, 18737
Wilkinson, M. H. 1998, J. Geophys. Res., 103, E9, 19985
Wright, A. N. 1987, J. Geophys. Res., 92, A9, 9963
Wright, A. N., & Smith, P. R. 1990, J. Geophys. Res., 95, A4, 3745
Zarka, P. 1998, J. Geohys. Res., 103, E9, 20159

Table 1. Used Nancay spectra of Io-related DAM.

Date [dd/mm/yy]	UT [hh mm]	f [MHz]	Polari–zation[a]	Storm type[b]
27/11/1990	01 : 02–03 : 59	16.0–25.5	RH	A
03/01/1991	04 : 55–06 : 00	15.0–24.8	RH	A
04–05/01/1991	23 : 30–01 : 20	15.0–21.2	LH	C
11–12/01/1991	23 : 35–02 : 43	15.5–23.3	LH	C
13/01/1991	01 : 28–03 : 00	13.5–34.3	RH	B
20/01/1991	00 : 13–03 : 59	13.0–29.8	RH	B
01/01/1992	01 : 00–02 : 58	12.4–19.0	LH	C
07–08/01/1992	23 : 54–01 : 09	20.0–27.7	RH	A
23/01/1992	03 : 58–07 : 17	21.2–25.1	RH	B
07/02/1992	05 : 29–06 : 24	19.7–33.5	RH	A
26/01/1993	04 : 10–05 : 13	17.0–24.2	RH	A
02/02/1993	05 : 00–06 : 16	15.3–27.8	RH	A
05/02/1993	00 : 47–01 : 47	20.0–30.0	RH	B
04/02/1993	01 : 29–02 : 03	10.0–19.5	LH	C
12/02/1993	01 : 00–03 : 17	15.3–24.0	RH	B
06/03/1993	01 : 15–02 : 43	17.0–28.3	RH	A
13/03/1993	01 : 50–03 : 14	15.2–26.2	RH	A
20/03/1993	02 : 45–03 : 45	19.9–31.5	RH	A
16/02/1994	01 : 56–02 : 54	14.9–24.0	RH	A
02/03/1994	02 : 33–03 : 45	19.8–29.1	RH	A
09/03/1994	03 : 15–04 : 45	17.1–27.5	RH	A
02/04/1994	22 : 38–23 : 49	19.5–27.3	RH	A
10/04/1994	23 : 37–01 : 00	16.2–27.2	RH	A
17/04/1994	01 : 50–04 : 41	15.3–22.5	LH	C
06/04/1995	01 : 01–02 : 24	19.1–25.5	RH	A
06/04/1995	02 : 53–05 : 15	15.0–23.0	LH	C
13/04/1995	01 : 37–02 : 24	16.3–29.0	RH	A
13/04/1995	04 : 24–06 : 03	15.5–23.2	LH	C
14/04/1995	03 : 43–06 : 20	21.3–29.8	RH	B
07–08/05/1995	23 : 43–00 : 58	15.3–19.8	LH	C
15/05/1995	01 : 07–02 : 33	15.4–23.8	LH	C
23/05/1995	00 : 55–03 : 25	20.8–28.5	RH	B
03/05/1996	01 : 23–02 : 41	15.3–20.6	LH	C
10/05/1996	02 : 20–04 : 10	15.8–24.0	LH	C
11/05/1996	02 : 52–04 : 32	17.5–31.0	RH	B
18/05/1996	03 : 49–05 : 11	18.1–24.3	RH	B
02/06/1996	02 : 20–03 : 18	15.5–22.0	RH	A
09/06/1996	03 : 49–04 : 49	17.9–27.7	RH	A
19/09/1996	17 : 42–18 : 08	19.9–26.1	RH	A
15/06/1997	01 : 55–02 : 55	15.5–20.5	RH	B
30/06/1997	00 : 08–01 : 52	19.5–28.0	RH	A
07/07/1997	00 : 57–03 : 17	18.9–26.0	RH	A
14/07/1997	01 : 55–03 : 12	22.1–30.3	RH	A
14/08/1997	21 : 59–23 : 38	20.8–26.4	RH	A
21–22/08/1997	22 : 30–00 : 18	19.9–29.2	RH	A
10/07/1998	03 : 20–04 : 37	21.1–31.0	RH	A
17/07/1998	03 : 58–05 : 06	22.0–28.8	RH	A
19/08/1998	03 : 47–04 : 52	17.6–29.3	RH	B
26/08/1998	03 : 23–04 : 13	17.3–24.8	RH	B
19–20/09/1998	22 : 53–02 : 45	15.0–33.0	RH	B
08/08/1999	03 : 38–05 : 30	18.5–35.1	RH	B
15/08/1999	04 : 04–07 : 01	22.2–30.8	RH	B
30/08/1999	04 : 25–05 : 39	19.8–28.2	RH	A
06/09/1999	05 : 14–07 : 03	21.8–27.5	RH	A
09/09/1999	00 : 06–02 : 52	21.8–35.0	RH	B
16/09/1999	00 : 27–04 : 17	16.0–30.8	RH	B
23/09/1999	02 : 48–04 : 24	12.3–22.9	RH	B
01/10/1999	01 : 02–03 : 43	15.8–25.5	RH	A
08/10/1999	01 : 28–03 : 50	19.8–34.8	RH	A
10/10/1999	21 : 06–22 : 48	21.8–33.4	RH	B
17/10/1999	21 : 43–23 : 51	18.0–33.0	RH	B
19/09/2000	01 : 48–04 : 40	15.8–25.0	RH	A
26/09/2000	02 : 13–04 : 45	15.8–28.1	RH	A
03/10/2000	03 : 28–05 : 04	18.0–31.0	RH	A
17/10/2000	04 : 37–05 : 50	19.6–30.2	RH	A
27/10/2000	23 : 05–23 : 56	18.7–26.7	RH	A
03–04/11/2000	23 : 23–01 : 31	20.0–32.5	RH	A
11/11/2000	00 : 08–02 : 25	19.5–31.0	RH	A
18/11/2000	00 : 42–02 : 37	20.0–27.9	RH	A
19/11/2000	02 : 38–04 : 19	19.5–29.5	RH	B
31/10/2001	00 : 41–03 : 22	19.3–33.5	RH	A
07/11/2001	01 : 31–03 : 15	18.2–31.8	RH	A
14/11/2001	02 : 07–05 : 08	19.3–30.0	RH	A
15/11/2001	02 : 55–05 : 26	17.3–31.0	RH	B
10/12/2001	00 : 07–02 : 11	18.8–35.5	RH	B
24/12/2001	00 : 40–02 : 36	17.8–30.8	RH	B
24/12/2001	03 : 16–04 : 36	17.4–26.0	RH	B
05/12/2002	01 : 20–03 : 38	17.0–21.4	LH	C
13/12/2002	03 : 51–05 : 25	18.0–27.3	RH	B
20/12/2002	02 : 55–05 : 30	18.0–27.5	RH	B
28/12/2002	02 : 49–04 : 03	17.8–31.6	RH	A
04/01/2003	03 : 38–05 : 13	18.0–28.8	RH	A
11/01/2003	04 : 06–05 : 43	19.3–33.5	RH	A
20/01/2003	22 : 10–23 : 48	17.6–28.3	RH	B
21/01/2003	00 : 13–01 : 20	20.5–26.0	RH	B
31/12/2003	05 : 00–06 : 35	18.1–29.0	RH	A
07/01/2004	05 : 35–07 : 14	18.7–29.0	RH	A
09/01/2004	00 : 27–02 : 42	17.0–21.8	LH	C
10/01/2004	01 : 01–02 : 43	15.0–27.4	RH	B
01/02/2004	01 : 05–02 : 01	19.5–28.3	RH	A
08/02/2004	01 : 43–03 : 43	17.0–28.3	RH	A
15/02/2004	02 : 38–04 : 15	17.0–28.1	RH	A
11/03/2004	01 : 08–03 : 13	15.2–21.5	LH	C
04/01/2005	02 : 45–04 : 33	14.0–21.0	LH	C
27/01/2005	02 : 38–03 : 36	12.2–26.8	RH	A
03/02/2005	03 : 24–04 : 47	15.5–26.7	RH	A
10/02/2005	03 : 46–05 : 40	16.3–28.5	RH	A
10/02/2005	05 : 45–07 : 40	18.0–25.0	LH	C
27–28/02/2005	22 : 33–00 : 13	17.9–28.6	RH	A
06–07/03/2005	23 : 23–01 : 06	18.5–28.2	RH	A
13–14/03/2005	23 : 57–01 : 30	17.5–28.2	RH	A
14/03/2005	02 : 07–04 : 36	15.7–22.5	LH	C
06/02/2006	05 : 20–06 : 49	20.8–30.8	RH	A
10–11/04/2006	23 : 53–02 : 23	15.4–25.0	LH	C
18/04/2006	00 : 40–03 : 30	15.5–23.3	LH	C
19/04/2006	02 : 10–03 : 15	19.5–29.5	RH	B
07/04/2007	01 : 41–03 : 54	14.4–24.4	LH	C

Table 1. continued.

[a] RH and LH are the right-hand and left-hand polarization channels respectively. [b] Io-A, Io-B, and Io-C are the standard terms (see Carr et al. 1983).